Journal of Solid State Chemistry 183 (2010) 3010–3016

Contents lists available at ScienceDirect

Journal of Solid State Chemistry

journal homepage: www.elsevier.com/locate/jssc

Synthesis and structural characterization of different topological coordination polymers based on tunable $Cu_4Br_{4-m}I_m$ secondary building units and macrocyclic azacalixaromatics

Li-Xia Wang [a], Liang Zhao [b,*], De-Xian Wang [a], Mei-Xiang Wang [a,b,*]

[a] Beijing National Laboratory for Molecular Sciences, CAS Key Laboratory of Molecular Recognition and Function, Institute of Chemistry, Chinese Academy of Sciences, Beijing 100190, China

[b] The Key Laboratory of Bioorganic Phosphorus Chemistry & Chemical Biology (Ministry of Education), Department of Chemistry, Tsinghua University, Beijing 100084, China

ARTICLE INFO

Article history:
Received 23 July 2010
Received in revised form
4 October 2010
Accepted 11 October 2010
Available online 16 October 2010

Keywords:
Coordination network
Macrocyclic ligand
Copper halide
Luminescence

ABSTRACT

The coordination self-assembly between the macrocyclic ligand tetraazacalix[4]pyrimidine (TAPM) with cubane-like copper halides (Cu_4X_4) produced five coordination polymers **1**–**5** $\{Cu_4Br_{4-m}I_m(TAPM)\}_n$ ($m=0$ (**1**), 1 (**2**), 2 (**3**), 3 (**4**) and 4 (**5**)). X-ray single crystal analysis revealed that the Br:I ratio in the Cu_4X_4 cores serves as a controlling factor to fine-tune the geometries of Cu_4X_4 and therefore induce the conformation variation of tetraazacalix[4]pyrimidine. Consequently, two different topological nets, *dia* and *lcs*, were successfully constructed based on tetrahedrally coordinated Cu_4X_4 secondary building units and the flexible macrocyclic quadridentate ligand TAPM. The structure details of **1**–**5** as porous materials are analyzed, which shows a solvent accessible volume within the range of 27 – 35%. Compounds **1**–**5** exhibit luminescence properties with the peak maximum at around 476 – 488 nm.

1. Introduction

The past two decades have witnessed tremendous development of the successful synthesis and characterization of a plethora of multi-dimensional coordination polymers [1], mostly constructed from modular synthesis of readily available metal ions or metal clusters and appropriate predesigned functional bridging organic ligands to impart unique properties for a wide range of potential applications including photonics [2], gas storage [3], sensing [4], separations [5] and catalysis [6]. The introduction of the 'secondary building unit (SBU)' [7] model has greatly facilitated better comprehension of acquired sophisticated structures and consequently implemented systematic design and synthesis of related materials. So far immense endeavors have been paid on the modification of organic spacer ligands, thus achieving isostructual materials with different sizes or containing versatile functionalities [8]. However, although a wealth of SBUs have been explored in diverse coordination architectures [9], the role of fine-tuning the geometry of SBU in manipulating the architectures of coordination polymers is rarely investigated until now.

Recently, the coordination polymeric materials based on copper(I) halides (CuX) and polydentate ligands have been of extensive interest because of their promising photophysical properties [10] and the abundance of various secondary building units (SBUs) derived from copper halides, such as rhomboid Cu_2X_2 dimers [11], cubane- or chair-like $[Cu_4X_4]$ tetramers, [10c–f,12], zigzag $[CuX]_n$ or $[Cu_3X_4]_n^{n-}$ chains [13], ladder or ribbon $[Cu_2I_2]_n$ chains [14], and two-dimensional (2D) $[CuI]_n$ layers [15]. In particular, the cubane-like Cu_4X_4 cluster serving as a four-connecting tetrahedral node has been frequently utilized in combination with linear ditopic or stelliform quadridentate ligands to build up three-dimensional (3D) quartz and diamond coordination structures [10c–f,16]. Scrutiny of structural details of reported Cu_4X_4-contained coordination polymers [10,16] indicates that halogen atoms always have significant effects on the attractive Cu · · · Cu interactions and the luminescent behavior of these materials due to the differential atom radii and electron negativities of Cl, Br and I [17]. We thus envisioned that mixing different halogen atoms in an integrated $Cu_4X_mX'_{4-m}$ (X, X' = halogen atoms) cluster in variable ratios may be capable of not only gradually tailoring the geometries of Cu_4X_4 secondary building units (SBUs) and thus the topologies of the whole coordination network structures, but affecting on photophysical behaviors of resulting coordination polymeric materials. Here, a series of five copper halide coordination complexes of the macrocyclic azacalixaromatic ligand tetraazacalixpyrimidine (TAPM) have been synthesized and characterized structurally and photophysically: $\{Cu_4Br_{4-m}I_m(TAPM)\}_n$ ($m=0$ (**1**), 1 (**2**), 2 (**3**), 3 (**4**) and 4 (**5**)),

* Corresponding author at: Tsinghua University, The Key Laboratory of Bioorganic Phosphorus Chemistry & Chemical Biology (Ministry of Education), Department of Chemistry, Beijing 100084, China. Fax: +86 10 62796761.
E-mail addresses: zhaolchem@mail.tsinghua.edu.cn (L. Zhao), wangmx@mail.tsinghua.edu.cn (M.-X. Wang).

0022-4596/$ - see front matter © 2010 Elsevier Inc. All rights reserved.
doi:10.1016/j.jssc.2010.10.011

wherein the Br/I ratio in the Cu_4X_4 cores serves as a controlling factor to induce the formation of two different topological *dia* and *lcs* networks Scheme 1.

2. Experimental

All chemicals purchased were of reagent grade and were used without further purification. Elemental analysis (C, H and N) was performed with a Carlo Erba 1106 elemental analyzer. Thermogravimetric (TG) behavior was investigated on a NETZSCH STA 409 PC/PG equipment. The luminescence property was measured on a Perkin–Elmer LS55 spectrometer.

2.1. Synthesis of complexes 1–5

{Cu_4Br_4(TAPM)}$_n$ **1**: Single crystals of **1** were prepared by layering a CH_3CN (2 ml) solution of CuBr (20 mg, 0.140 mmol) over a solution of TAPM (20 mg, 0.047 mmol) in CH_2Cl_2 (2 ml). Laurel-green crystals were isolated after 12 h (24.4 mg, 70%) (calculated with CuBr): Anal. Calcd. for $Cu_4Br_4C_{20}H_{20}N_{12}$: C, 23.97; H, 2.01; N, 16.77; found: C, 23.98; H, 2.08; N, 16.66.

{Cu_4Br_3I(TAPM)}$_n$ **2**: Single crystals of **2** were prepared by layering a solution of a mixture of CuBr (18 mg, 0.126 mmol) and CuI (2.4 mg, 0.013 mmol) in CH_3CN (2 ml) over a CH_2Cl_2 solution (2 ml) of TAPM (20 mg, 0.047 mmol). Laurel-green crystals were isolated after 12 h (17.0 mg, 71%) (calculated with CuI): Anal. Calcd. for $Cu_4Br_3IC_{20}H_{20}N_{12}$: C, 22.89; H, 1.92; N, 16.02; found: C, 22.73; H,1.96; N, 15.67.

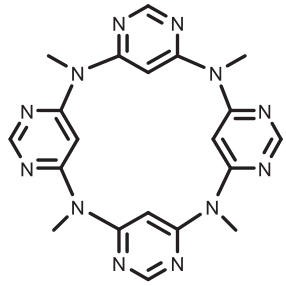

Tetraazacalix[4]pyrimidine (TAPM)

Scheme 1

{$Cu_4Br_2I_2$(TAPM)}$_n$ **3**. The synthesis method for **3** is the same as for **2** but uses different amounts of CuBr and CuI: CuI (5 mg, 0.026 mmol), CuBr (15 mg, 0.105 mmol) and TAPM (20 mg, 0.047 mmol). Laurel-green crystals of **3** were isolated after 12 h (15.0 mg, 65.7%) (calculated with CuI): Anal. Calcd. for $Cu_4Br_2I_2C_{20}H_{20}N_{12}$: C, 21.91; H, 1.84; N, 15.33; found: C, 21.69; H, 1.91; N, 14.83.

{Cu_4BrI_3(TAPM)}$_n$ **4**: The synthesis method for **4** is similar to that for **2**. The amounts were as follows: CuI (11.4 mg, 0.060 mmol), CuBr (8.6 mg, 0.060 mmol) and TAPM (20 mg, 0.047 mmol). Laurel-green crystals were deposited after 12 h (20.1 mg, 98%) (calculated with CuI): Anal. Calcd. for $Cu_4BrI_3C_{20}H_{20}N_{12}$: C, 21.01; H,1.76; N, 14.70; found: C, 21.07; H,1.93; N, 14.26.

{Cu_4I_4(TAPM)}$_n$ **5**: The method of synthesis of single crystals of **5** is similar to that of **1**. The amounts were as follows: CuI (20 mg, 0.105 mmol) and TAPM (20 mg, 0.047 mmol). Colorless crystals were isolated after 12 h (26.0 mg, 83%) (calculated with CuI): Anal. Calcd. for $Cu_4I_4C_{20}H_{20}N_{12}$: C, 20.18; H,1.69; N, 14.12; found: C, 19.64; H,1.87; N, 14.09.

2.2. X-ray crystallographic analysis

Data for complexes **1**–**5** were collected at 173 K with Mo$K\alpha$ radiation (λ=0.73073 Å) on a Rigaku Saturn 724+CCD diffractometer with frames of oscillation range 0.5°. All structures were solved by direct methods, and non-hydrogen atoms were located from difference Fourier maps. All non-hydrogen atoms were subjected to anisotropic refinement by full-matrix least-squares on F^2 by using the SHELXTL program. The crystal data and X-ray structure refinement parameters are summarized in Table 1. Solvent molecules in the structures of complexes **1**–**5** were highly disordered and were impossible to refine using conventional discrete-atom models. Therefore, the contribution of solvent electron density was eventually removed using the SQUEEZE routine in PLATON [18], producing a set of solvent-free diffraction intensities. The final formulae of **1**–**5** were calculated from the SQUEEZE results in combination with those of elemental analyses. CCDC-765684–765688 (**1**–**5**, respectively) contain the supplementary crystallographic data for this paper, obtainable free of charge from The Cambridge Crystallographic Data Centre at http://www.ccdc.cam.ac.uk/data_request/cif. All figures are drawn by using X-seed program [19].

Table 1
Crystallographic data of complexes **1**–**5**.

	Compound				
	1	**2**	**3**	**4**	**5**
Empirical formula	$C_{20}H_{20}Br_4Cu_4N_{12}$	$C_{20}H_{20}Br_3ICu_4N_{12}$	$C_{20}H_{20}Br_2I_2Cu_4N_{12}$	$C_{20}H_{20}BrI_3Cu_4N_{12}$	$C_{20}H_{20}I_4Cu_4N_{12}$
M_r	1002.28	1049.26	1096.26	1143.26	1190.26
Crystal system	Tetragonal	Tetragonal	Cubic	Cubic	Tetragonal
Space group	*I*-4	*I*-4	*I*-43*d*	*I*-43*d*	*I*-4
a (Å)	13.298(2)	13.286(1)	23.020(3)	23.110(1)	12.669(2)
b (Å)	13.298(2)	13.286(1)	23.020(3)	23.110(1)	12.669(2)
c (Å)	9.944(2)	10.052(1)	23.020(3)	23.110(1)	11.982(2)
V (Å^3)	1758.4(5)	1774.5(2)	12199(2)	12 341.8(9)	1923.1(5)
ρ (g/cm^3)	1.893	1.946	1.786	1.851	2.055
Z	2	2	12	12	2
R_1 ($I>2\sigma(I)$)[a]	0.0341	0.0379	0.0531	0.0597	0.0303
wR_2(all data)[b]	0.1062	0.1108	0.1689	0.1556	0.0825
GOF	1.182	1.129	1.084	1.039	1.100

[a] $R_1=\sum||F_o|-|F_c||/\sum|F_o|$.
[b] $wR_2=\{\sum[w(F_o^2-F_c^2)^2]/\sum[w(F_o^2)^2]\}^{1/2}$.

3. Results and discussion

3.1. Synthesis and crystal structures

In contrast to the hydro(solvo)thermal synthetic methods for most reported Cu_4X_4 coordination polymers [12,17], complexes **1**–**5** were easily obtained by diffusing the acetonitrile solution of single or mixed copper(I) halide(s) into the CH_2Cl_2 solution of TAPM. Since the crystals of the Cu_4I_4 complex were easily deposited, other halide-mixed complexes $\{Cu_4Br_{4-m}I_m(TAPM)\}_n$ (m=1 (**2**), 2 (**3**), 3 (**4**)) were synthesized by use of the mixed solution of CuBr/CuI in the high ratio of 10:1, 4:1, and 1:1, respectively. The cyclic tetratopic ligand, tetraazacalix[4]pyrimidine (TAPM) was designedly synthesized through the fragment coupling protocol between *N*,*N*′-dimethyl-4,6-pyrimidinediamine and 4,6-dichloropyrimidine [20], for the purpose of acquiring sophisticated multidimensional materials with a higher degree of porosity. Compared with chain-like organic ligands that favorably lead to the formation of interpenetrated networks, the macrocyclic scaffold of TAPM may avoid the occurrence of interpenetration because of constrained coordination sites and steric effect.

X-ray crystallographic analysis revealed that **1**, **2** and **5** are isostructural (structure **A**) and crystallize in the tetragonal space group of *I*-4 (No. 82), whereas isostructural complexes **3** and **4** (structure **B**) have a higher cubic symmetry of *I*-43*d* (No. 220). It is notable that complex **5** $\{Cu_4I_4(TAPM)\}_n$ has a Flack parameter of 0.42(4), suggestive of a twinned crystal of **5**. The Br/I ratios in the $Cu_4Br_{4-m}I_m$ SBUs in **2**, **3** and **4** were initially assigned by structure refinements. For example, the bromide and iodide atoms in complex **3** can be differentiated as two parts in a 0.48:0.52 occupancy ratio at the same position on the Fourier difference map according to refinement by using the SHELXTL program. Such Br/I proportions in **2**–**4** were further confirmed by elemental analysis as shown in Table 2.

Fig. 1 shows the unsymmetrical unit in **1**–**5** each involves a copper(I) atom, a halogen atom and a quarter part of TAPM. The unit cell volume of complexes **3** and **4** is approximately 12 000 Å^3, sixfold of the volume of complexes **1**, **2** and **5**. Therefore, the Z value for complexes **3** and **4** is 12 while that value for complexes **1**, **2** and **5** is 2. Each TAPM ligand bonds to four Cu_4X_4 clusters by use of four nitrogen atoms on the pyrimidine rings. In the Cu_4X_4 cores of **1**–**5**, four symmetry equivalent copper atoms constitute a quasi-tetrahedron, where each of its faces is capped by a halogen atom. Viewed along the S_4-axis in every complex, such tetrahedron can be projected as an equilateral (L_1) distorted tetragon, wherein the identical length of its two diagonals is denoted as L_2. The selected distances and angles of the Cu_4X_4 cores in **1**–**5** (Table 3) suggest that the Br/I ratio is indeed a controlling factor to adjust the cuprophilic interactions as well as the geometry of Cu_4X_4 clusters. As listed in Table 3, the two peripheral Cu–X distances (L_4 and L_5) in complexes **1**, **2** and **5** are comparable with a distance deviation lower than 0.02 Å. In this way, the Cu_4X_4 cores in **1**, **2** and **5** are highly symmetric, which is consistent with the fact that four identical halide atoms are involved in **1** and **5** and that the metal cluster core of complex **2** has a high ratio of single halide. However, a discernible difference of 0.1 Å between L_4 and L_5 occurs in complexes **3** and **4**, which leads to the distortion of the whole cluster as shown in Fig. S1 in the Supporting Information.

With increase in iodide proportion from **1** to **4**, the Cu···Cu distances (L_1 and L_2) are shortened due to the absence of the cuprophilic interactions (longer than 2.80 Å, the sum of the van der Waals radii of copper atom) through weak interactions to moderate ones. Such an upward trend of the Cu···Cu interactions can be rationalized by the fact that the high electronegativity bromide atom weakens the electron density in the Cu *s*-orbitals that provide the bonding component of the cuprophilic interactions. It is notable that one Cu···Cu distance of L_2 in **5** is off such a trend and is tuned back to 2.77 Å, which is possibly due to the highly symmetric conformation of Cu_4I_4 and the longer atomic radius of iodine in contrast to bromine. In addition, in **3** and **4** L_2 is shorter than L_1, in contrast to the reverse scenario in the other three

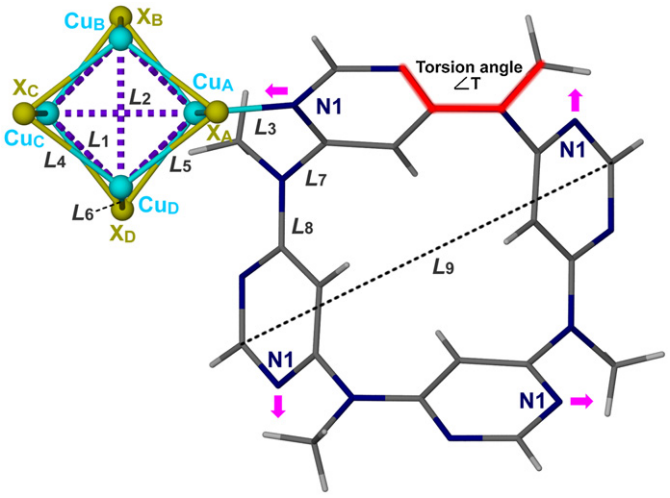

Fig. 1

Table 2
Elemental analysis results of **1**–**5**. The crystals of **1**–**5** were collected by filtration, washed with a little amount of CH_2Cl_2/CH_3CN, and dried under high vacuum at 120 °C for 36 h to give samples of **1**–**5** for elemental analysis.

Complex	Formula	Br/I occupancy ratio	Calculated	Found
1	$Cu_4Br_4C_{20}H_{20}N_{12}$		C 23.97	23.98
			H 2.01	2.08
			N 16.77	16.66
2	$Cu_4Br_3IC_{20}H_{20}N_{12}$	3.20:0.80	C 22.89	22.73
			H 1.92	1.96
			N 16.02	15.67
3	$Cu_4Br_2I_2C_{20}H_{20}N_{12}$	2.07:1.93	C 21.91	21.69
			H 1.84	1.91
			N 15.33	14.83
4	$Cu_4BrI_3C_{20}H_{20}N_{12}$	0.94:3.06	C 21.01	21.07
			H 1.76	1.93
			N 14.70	14.26
5	$Cu_4I_4C_{20}H_{20}N_{12}$		C 20.18	19.64
			H 1.69	1.87
			N 14.12	14.09

Table 3
Selected distances, bond lengths and angles in **1**–**5**.

Complex		**1**	**2**	**3**	**4**	**5**
Cu···Cu	L_1 (Å)	2.805(1)	2.793(1)	2.750(2)	2.746(2)	2.743(1)
	L_2 (Å)	2.932(1)	2.932(1)	2.652(2)	2.649(3)	2.774(1)
Cu–N	L_3 (Å)	2.025(4)	2.035(4)	2.058(7)	2.070(7)	2.064(5)
Cu–X	L_4 (Å)	2.491(1)	2.531(1)	2.620(2)	2.672(2)	2.649(1)
	L_5 (Å)	2.508(1)	2.545(1)	2.752(2)	2.774(2)	2.667(1)
	L_6 (Å)	2.612(1)	2.635(1)	2.556(1)	2.597(1)	2.731(1)
$\angle Cu_{(ABC)}{}^{-}{}_{(ADC)}$(deg.)		75.6	76.1	66.8	66.8	71.7
$(CH_3)N–C_{pym}$	L_7 (Å)	1.436(6)	1.426(7)	1.46(1)	1.45(1)	1.434(7)
	L_8 (Å)	1.346(6)	1.345(6)	1.39(1)	1.39(1)	1.347(7)
Upper-rim distance	L_9 (Å)	8.163	8.177	7.701	7.770	8.005
Torsion angle ∠T (deg.)		7.0	6.2	9.9	10.5	4.2

complexes, implying a severe curvature of the equilateral tetragon in **3** and **4**. This observation is also evidenced by the dihedral angles between two copper triangles, wherein the dihedral angle of 66.8° in **3** and **4** is smaller than the angles in **1**, **2** and **5**.

It is remarkable that the TAPM ligand in **1**–**5** can self-adjust its own conformation to complementarily adapt to the geometrical variation of Cu_4X_4 SBUs. Our previous studies on the structures of N-bridged calixarenes have shown that the bridging nitrogen atoms can adopt different electronic configurations and form various degrees of conjugation with their adjacent aromatic rings to resultantly tune the conformation and the cavity of azacalixarene ligands [21]. Compared with the conformation of TAPM in **1**, **2** and **5**, the degree of conjugation between the bridged N–CH_3 moiety and adjacent two pyrimidine rings is weakened in **3** and **4** as a result of (i) the elongation of two characteristic distances L_7 and L_8 and (ii) the deflection of the torsion angle $\angle T$. The upper-rim distance L_9 in **3** and **4** is shortened as well, similar to the curvature of the Cu_4X_4 tetrahedron therein. Such consecutive changes of TAPM may be ascribed to the fact that the variation of Cu_4X_4 SBUs induces the conformational tuning of TAPM considering precise recognition between the four-connecting acceptor (Cu_4X_4) and the quadridentate donor (TAPM).

The linkage of Cu_4X_4 SBUs and TAPM in the network structure **A** of **1**, **2** and **5** yields a two-dimensional (2D) coordination layer parallel to the *ab* plane (Fig. 2(a)) with Cu_4X_4 SBUs located at the upper and nether layers. A series of metallo-macrocycles (11.8 × 11.8 Å) are constructed by use of two linear bonding sites of Cu_4X_4 and four nitrogen coordination atoms of TAPM. Such coordination layers are further connected to adjacent ones with the linkage of the remaining two bonding sites of Cu_4X_4 to generate a three-dimensional (3D) coordination network. Viewed along the *a*-axis, these coordination layers are packed along the *c*-direction in the *ABAB* form (Fig.2(b)). In addition, structure **A** can be topologically referred to as a quasiregular 6^6 *dia* net with the long Schäfli symbol of $6_2.6_2.6_2.6_2.6_2.6_2$ as shown in Fig. 2(c) through abstracting the tetrahedral Cu_4X_4 unit and tetratopic TAPM ligand both as a four-connecting node. Herein, all vertices and edges are equivalent by symmetry but not all angles. Structure **A** involves a series of void cages (a solvent accessible volume of 26.6%, 27.7% and 30.5% in **1**, **2** and **5**, respectively) constructed through the connection of four Cu_4X_4 units by six TAPM ligands: two at upper and nether and the other four at peripheral (Fig. 3). The structure refinement found that highly disordered solvent molecules fill in these voids, which are squeezed.

Similar to the bonding fashion in structure **A**, structure **B** in complexes **3** and **4** is built as well from the four-connecting Cu_4X_4 SBUs and the quadridentate ligand TAPM. A trigonal anti-prism void cage is constructed by six Cu_4X_4 SBUs with the linkage of three TAPM ligands in a μ_3-mode at each terminal (Fig. 4(a)). Viewed along the [1 1 1] direction, such void cage is finite and discontinuous due to three bridging N–CH_3 moieties protruding inward into the cage (Fig. 4(b)). Undefined highly disordered solvent molecules are encapsulated in those void cages. A calculated solvent accessible volume of approximately 35% for **3** and **4** is achieved in the structure **B**. By analogy to the node selection in the above *dia* net of **A**, two distorted tetrahedral connectivity nodes are similarly acquired in 3D network structure **B** of **3** and **4**. The overall structure of **B** topologically possesses a *lcs* net with the short vertex symbol of 6^6; the long Schäfli symbol is $6.6.6_2.6_2.6_2.6_2$ (Fig. 5). Compared with the uniform six-membered chair-rings in the *dia* topological net of **A**, both chair-rings and boat-rings co-exist in the *lcs* topological net of **B** (Fig. S2).

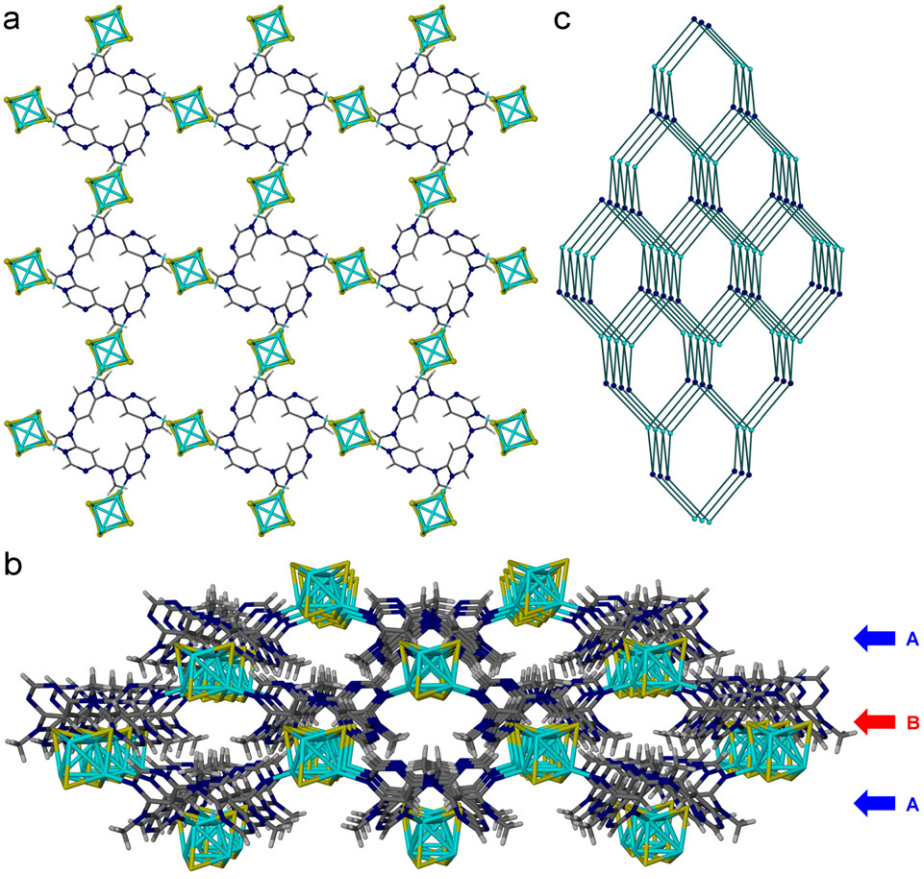

Fig. 2

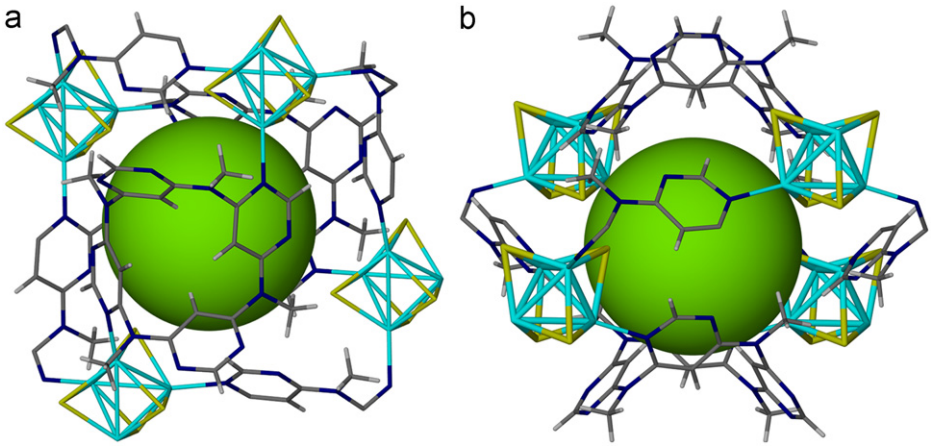

Fig. 3

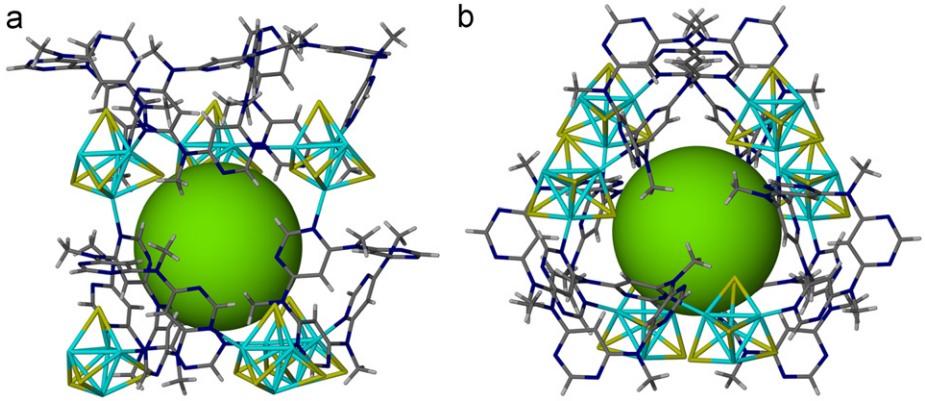

Fig. 4

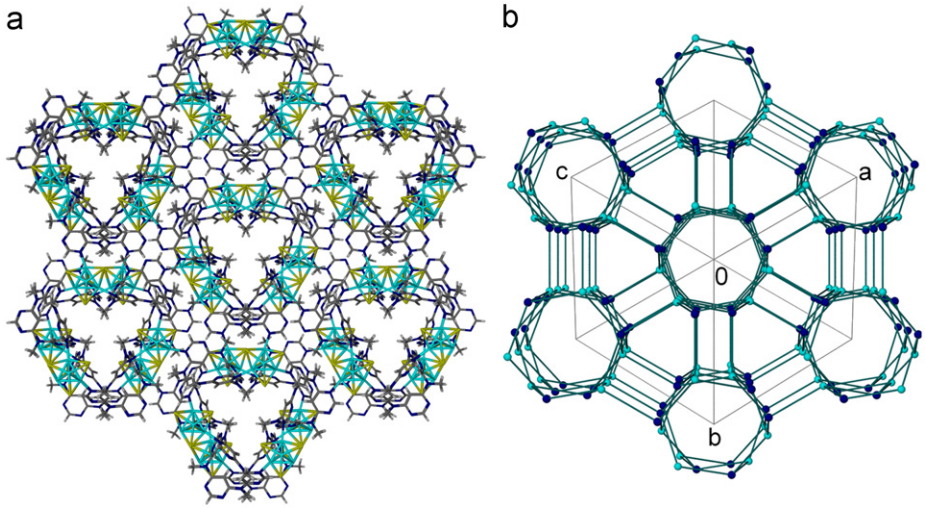

Fig. 5

In contrast to a solvent accessible volume of 6.2% in a reported triply interpenetrated network structure composed of Cu_4I_4 and a stelliform organic ligand tetrakis(4-pyridyloxymethylene)methane [16b], the higher degree of porosity of **1**–**5** substantiates our assumption that the macrocyclic ligand TAPM has an advantage over chain-like ligands in preventing interpenetration. Through tuning the geometry of the $Cu_4Br_{4-m}I_m$ secondary building units by varying the Br/I ratios, the conformation of TAPM and the whole of the coordination structures is modified as well, leading to two different topological *dia* and *lcs* nets.

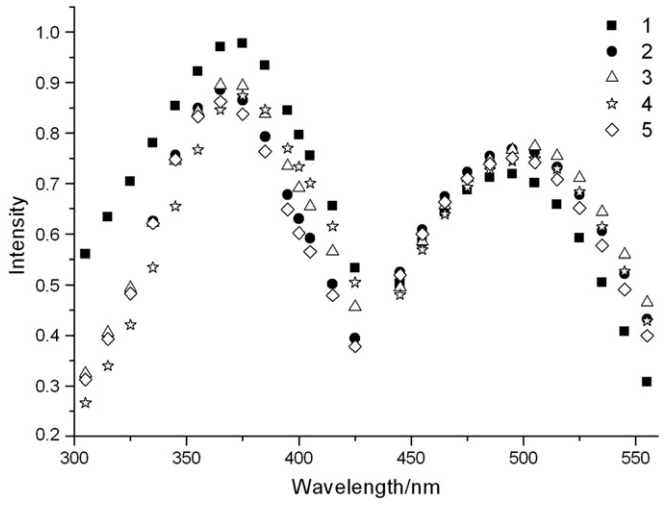

Fig. 6

3.2. Thermal analysis

Thermogravimetric analysis (TGA) was carried out in a nitrogen stream in the temperature range of 40–800 °C with a heating rate of 10 °C/min (Fig. S3). Compounds **1**–**5** all exhibit two steps of weight losses. At the first stage from about 200 to 260 °C, the TAPM ligand in **1**–**5** is partially pyrolyzed to an undefined species with the loss of approximately 10% of total formula weight. Finally, the loss of the organic ligands and I^- start to occur over 360 °C. The reason for the observation of two stages in the TG curve for **1**–**5** is the stepwise decomposition of the macrocyclic ligand TAPM.

3.3. Photoluminescent properties

The emission spectra of complexes **1**–**5** as solids were collected at room temperature with the excitation at $\lambda = 380$ nm (Fig. 6). A blue emission with peak maximum at around $476-488$ nm is observed for each complex, which was proposed to originate from the halogen-to-TAPM charge transfer (XLCT) by analogy to the high energy emission of $[Cu_4I_4(pyridine)_4]$ [13]. In addition, although the $Cu\cdots Cu$ distances of L_1 in **1**–**5** are varied systematically along with the variation of the Br:I ratio, the emission maxima of **1**–**5** proved to be rather insensitive to the nature of halogen atoms. This behavior may result from two counterpoised trends, namely the respective relative ionicities resulting from the electronegativity order ($Br > I$) balanced against the trend in ionization energies ($Br^- > I^-$) for the $X-Cu-TAPM$ system. Such small difference between complexes **1**–**5** due to variable Br/I ratio in $Cu_4Br_{4-m}I_m$ clusters is in sharp contrast to the discernible emission spectra of reported Cu*X*(2,3-dimethylpyrazine) compounds (X=Cl, Br, I), [22], which exhibit large emission maxima ($\Delta\lambda$) at around 20–30 nm.

3.4. Infrared spectra

As shown in Fig. S4 of the Supporting Information, the IR spectra of complexes **1**–**5** display no much difference. The asymmetrical and symmetrical stretching frequencies of the pyrimidine ring in the range 1600–1450 cm^{-1} are located at approximately the same positions in **1**–**5**, but are 10–20 cm^{-1} larger than the wave numbers of the corresponding vibrations in the TAPM ligand. This may be attributed to the conformation rigidity of TAPM after coordination self-assembly.

4. Conclusions

In conclusion, we have successfully achieved a series of five coordination polymers **1**–**5** with high degree of porosity by use of the macrocyclic quadridentate ligand TAPM and $Cu_4Br_{4-m}I_m$ SBUs, wherein TAPM can efficiently prevent the formation of interpenetrated structures. Through tuning of the geometry of the $Cu_4Br_{4-m}I_m$ secondary building units by varying the Br/I ratios, the conformation of TAPM and the whole coordination structures are modified as well, leading to two different topological *dia* and *lcs* nets. The thermal stability and photophysical properties of **1**–**5** are also investigated. This work offers a viable means to alter the Cu_4X_4 or halogen-related SBUs' geometries by simply changing halogen atom proportions, thus possibly constructing new multidimensional coordination networks.

Acknowledgments

We gratefully acknowledge the financial support from the National Natural Science Foundation of China and the Ministry of Science and Technology (2007CB808005).

Appendix A. Supporting information

Supplementary data associated with this article can be found in the online version at doi:10.1016/j.jssc.2010.10.011.

References

[1] R. Robson, J. Chem. Soc. Dalton Trans (2000) 3735;
B. Moulton, M.J. Zaworotko, Chem. Rev. 101 (2001) 1629;
S.R. Batten, Curr. Opin. Solid State Mater. Sci. 5 (2001) 107;
N.L. Rosi, M. Eddaoudi, J. Kim, M. O'Keeffe, O.M. Yaghi, Cryst. Eng. Commun. 4 (2002) 410;
C. Janiak, Dalton Trans. (2003) 2781;
S. Kitagawa, K. Uemura, Chem. Soc. Rev. 34 (2005) 109;
A.K. Cheetham, C.N.R. Rao, R.K. Feller, Chem. Commun. (2006) 4780;
M. Hong, Cryst. Growth Des 7 (2007) 10;
J.J. Vittal, Coord. Chem. Rev. 251 (2007) 1781;
J.P. Zhang, X.C. Huang, X.M. Chen, Chem. Soc. Rev 38 (2009) 2385;
W. Lin, J.W. Rieter, K.M.L. Taylor, Angew. Chem. Int. Ed. 48 (2009) 650.
[2] R. Evans, W. Lin, Acc. Chem. Res. 35 (2002) 511.
[3] N.L. Rosi, J. Eckert, M. Eddaoudi, D.T. Vodak, J. Kim, M. O'Keeffe, O.M. Yaghi, Science 300 (2003) 1127;
B. Chen, X. Zhao, A. Putkham, K. Hong, E.B. Lobkovsky, E.J. Hurtado, A.J. Fletcher, K.M. Thomas, J. Am. Chem. Soc. 130 (2008) 6411;
L.J. Murray, M. Dincă, J.R. Long, Chem. Soc. Rev. 38 (2009) 1294.
[4] B.L. Chen, L.B. Wang, F. Zapata, G.D. Qian, E.B. Lobkovsky, J. Am. Chem. Soc. 130 (2008) 6718.
[5] Y.S. Bae, O.K. Farha, A.M. Spokoyny, C.A. Mirkin, J.T. Hupp, R.Q. Snurr, Chem. Commun (2008) 4135;
J.R. Li, R.J. Kuppler, H.C. Zhou, Chem. Soc. Rev. 38 (2009) 1477.
[6] D.N. Dybtsev, A.L. Nuzhdin, H. Chun, K.P. Bryliakov, E.P. Talsi, V.P. Fedin, K. Kim, Angew. Chem. Int. Ed. 45 (2006) 916;
S.H. Cho, B.Q. Ma, S.T. Nguyen, J.T. Hupp, T.E. Albrecht-Schmitt, Chem. Commun. (2006) 2563;
C. Wu, W. Lin, Angew. Chem. Int. Ed 46 (2007)1075 46 (2007).
[7] M. Eddaoudi, D.B. Moler, H. Li, B. Chen, T.M. Reineke, M. O'Keeffe, O.M. Yaghi, Acc. Chem. Res. 34 (2001) 319.
[8] Z. Wang, S.M. Cohen, Chem. Soc. Rev. 38 (2009) 1315 and references therein.
[9] D.J. Tranchemontagne, J.L. Mendoza-Cortés, M. O'Keeffe, O.M. Yaghi, Chem. Soc. Rev. 38 (2009) 1257.
[10] (a) P.C. Ford, E. Cariati, J. Bourassa, Chem. Rev. 99 (1999) 3625;
(b) M. Vitale, P.C. Ford, Coord. Chem. Rev. 219-221 (2001) 3;
(c) S. Hu, M.L. Tong, Dalton Trans. (2005) 1165;
(d) M. Sarka, K. Biradha, Chem. Commun. (2005) 2229;
(e) T.H. Kim, Y.W. Shin, J.H. Jung, J.S. Kim, J. Kim, Angew. Chem. Int. Ed. 47 (2008) 685;
(f) L.L. Li, H.X. Li, Z.G. Ren, D. Liu, Y. Chen, Y. Zhang, J.P. Lang, Dalton Trans. (2009) 8567.
[11] (a) S.Y. Lee, S. Park, S.S Lee, Inorg. Chem. 48 (2009) 11335;
(b) G.F. Manbeck, W.W. Brennessel, C.M Evans, R. Eisenberg, Inorg. Chem. 49 (2010) 2834.
[12] (a) C.L Raston, A.H. White, J. Chem. Soc. Dalton Trans. (1976) 2153;
(b) V. Schramm, Cryst. Commun.Struct. 11 (1982) 1549.

[13] (a) P.M. Graham, R.D. Pike, M. Sabat, R.D. Bailey, W.T. Pennington, Inorg. Chem. 39 (2000) 5121;
(b) J.K. Cheng, Y.G. Yao, J. Zhang, Z.J. Li, Z.W. Cai, X.Y. Zhang, Z.N. Chen, Y.B. Chen, Y. Kang, Y.Y. Qin, Y.H. Wen, J. Am. Chem. Soc. 126 (2004) 7796;
(c) F. Thébault, S.A. Barnett, A.J. Blake, C. Wilson, N.R. Champness, M. Schröder, Inorg. Chem. 45 (2006) 6179.
[14] G.H. Li, Z. Shi, X.M. Liu, Z.M. Dai, S.H. Feng, Inorg. Chem. 43 (2004) 6884.
[15] (a) A.J. Blake, N.R. Brooks, N.R. Champness, P.A. Cooke, A.M. Deveson, D. Fenske, P. Hubberstey, W.S. Li, M. Schröder, J. Chem. Soc. Dalton Trans. (1999) 2103;
(b) R. Peng, T. Wu, D. Li, Cryst. Eng. Comm. 7 (2005) 595.
[16] (a) Y. Chen, H.X. Li, D. Liu, L.L. Liu, N.Y. Li, H.Y. Ye, Y. Zhang, J.P Lang, Cryst. Growth Des. 8 (2008) 3810;
(b) S.B Ren, L. Zhou, J. Zhang, Y.Z. Li, H.B. Du, X.Z. You, Cryst. Eng. Commun. 11 (2009) (1834).
[17] M. Vitale, C.K. Ryu, W.E. Palke, P.C. Ford, Inorg. Chem. 33 (1994) 561.
[18] A.L. Spek, J. Appl. Crystallogr. 36 (2003) 7.
[19] L.J. Barbour, J. Supramol. Chem. 1 (2001) 189;
J.L. Atwood, L.J. Barbour, Cryst. Growth Des. 3 (2003) 3.
[20] L.X. Wang, D.X. Wang, Z.T. Huang, M.X. Wang, J. Org. Chem. 75 (2010) 741.
[21] M.X. Wang, Chem. Commun. (2008) 4541.
[22] I. Jeβ, P. Taborsky, J. Pospíšil, C. Nather, Dalton Trans. (2007) 2263.